IEEE Access
Multidisciplinary | Rapid Review | Open Access Journal

Received 10 July 2023, accepted 10 August 2023, date of publication 14 August 2023, date of current version 18 August 2023.

*Digital Object Identifier 10.1109/ACCESS.2023.3305251*

RESEARCH ARTICLE

# Low-Profile Dual-Polarized Composite Patch-Monopole Antenna With Broadband and Widebeam Characteristics

**SON XUAT TA[1], (Member, IEEE), THANH TUNG PHUNG[1], KHAC KIEM NGUYEN[1], (Member, IEEE), CHIEN DAO-NGOC[1], (Senior Member, IEEE), AND NGHIA NGUYEN-TRONG[2], (Senior Member, IEEE)**

[1]School of Electrical and Electronic Engineering, Hanoi University of Science and Technology, Hanoi 100000, Vietnam
[2]School of Electrical and Electronic Engineering, The University of Adelaide, Adelaide, SA 5005, Australia

Corresponding author: Son Xuat Ta (xuat.tason@hust.edu.vn)

This work was supported by the Ministry of Science and Technology (MOST) of Vietnam under Grant NDT/KR/23/11.

**ABSTRACT** This paper presents a low-profile, high-isolation, dual-polarized antenna with broadband and widebeam characteristics. The antenna consists of a square patch fed by double differential-fed scheme for the high-isolation dual-polarized radiation. The patch is loaded with four top-hat monopoles to not only broaden the beamwidth, but also generate an extra resonance, which is utilized to improve the operational bandwidth. For verification, an antenna prototype with $0.096\lambda_0$-height at the center frequency of 2.5 GHz has been fabricated and measured. The measurements result in a 10-dB return loss bandwidth of 13.8% (2.36 - 2.71 GHz), an isolation of $\geq$ 43 dB, and excellent widebeam dual-polarized radiation, i.e., at 2.4 - 2.6 GHz, its half-power beamwidths are $\geq 180°$ and $\geq 120°$ in the E- and H-planes, respectively.

**INDEX TERMS** Composite patch-monopole, top-hat monopole, widebeam, dual-polarization, broadband, high isolation.

## I. INTRODUCTION

In order to achieve the optimal operation, several modern wireless communication systems, such as indoor communications, short-range automotive radars, mobile communications, and wide-angle scanning phased arrays, require antennas with widebeam radiation, e.g., half-power beamwidths (HPBWs) are normally expected to be $\geq 120°$ [1]. Typical radiators such as microstrip patches, printed dipoles or crossed dipoles, yield HPBWs of approximately $60° - 70°$, which are insufficient to meet the above requirement. Accordingly, different techniques are required to enlarge their beamwidths. Those techniques, for instance, include patch-monopole composite [2], [3], [4], [5], angled dipoles [6], [7], [8], [9], dipole-monopole composite [10], [11], [12], microstrip magnetic dipoles [13], capacitive via fence [14], using fusion modes of dielectric resonator antennas [15], loading high-permittivity dielectric slabs and using folded ground plane [16], current cancellation method [17], and utilizing metallic walls [18], [19], [20], [21]. Most of the aforementioned techniques yield negligible or negative effects on the bandwidth of the original structures. Furthermore, most of these widebeam antennas exhibit a high profile of around $0.2\lambda_c$ ($\lambda_c$ is the free space wavelength at the center frequency).

In this paper, a square patch antenna is symmetrically loaded with four top-hat monopoles to achieve: low-profile structure, large beamwidth and broad bandwidth simultaneously. The two out-of-phase currents on two monopoles induced by the patch are radiating together with two patch's equivalent magnetic currents to provide widebeam characteristics. The monopoles generate an extra resonance, which is combined with the patch resonance to enlarge the bandwidth. Finally, the structure symmetry is utilized with a double differential-fed scheme to achieve a high-isolation dual-polarized radiation.

The associate editor coordinating the review of this manuscript and approving it for publication was Wanchen Yang.

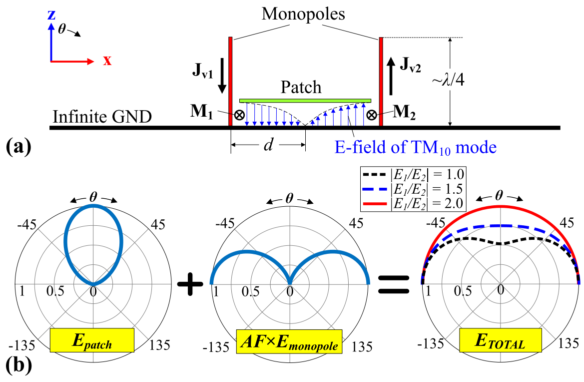


**FIGURE 1.** **(a) Initial design (with high profile) of the composite patch-monopole antenna; (b) its synthesis radiation pattern in the E-plane (in linear-scale).**

## II. ANTENNA DESIGN AND CHARACTERISTICS

### A. INITAL DESIGN CONCEPT

The composite patch-monopole is a simple technique to broaden HPBW of the microstrip patch antennas [2], [3], [4], [5]. Fig. 1(a) shows the initial design concept. It consists of a rectangular patch, two $\sim\lambda/4$ monopoles, and an infinite ground plane (GND). The patch is designed to operate at the fundamental $TM_{10}$ mode. The radiated field of the patch ($E_{\text{patch}}$) is caused by two equivalent magnetic currents ($M_1$ and $M_2$) and can be expressed in E-plane as [22]

$$E_{\text{patch}}(\theta) \approx E_1 \cos(\frac{\beta L}{2} \sin\theta) \tag{1}$$

where $\beta$ is the propagation constant in free space, $L$ is the patch length, and $E_1$ is the complex amplitude. The monopoles are excited by the coupling from the patch. When the patch is excited at the $TM_{10}$ mode, the two vertical currents ($J_{v1}$ and $J_{v2}$) have the same amplitude and opposite phase due to symmetry. A $\lambda/4$-monopole on infinite ground plane has the E-plane radiated field as [22]

$$E_{\text{monopole}}(\theta) = E_2 \frac{\cos(\frac{\pi}{2}\cos\theta)}{\sin\theta} \tag{2}$$

where $E_2$ is the complex amplitude. The ratio $E_1/E_2$ is mainly determined by the coupling between the patch and monopoles. The array factor of these two monopoles is

$$AF_{\text{monopole}}(\theta, \phi) = 2\sin(\beta d \sin\theta \cos\phi) \tag{3}$$

The total field of the composite patch-monopole antenna is

$$E_{\text{TOTAL}} = E_{\text{patch}} + E_{\text{monopole}} \times AF_{\text{monopole}} \tag{4}$$

Fig. 1(b) shows the calculated E-plane ($\phi = 0^\circ$) normalized pattern of the antenna ($d = \lambda/4$). It can be observed that the ratio between the amplitudes of $E_{\text{patch}}$ and $E_{\text{monopole}}$, i.e., $|E_1/E_2|$ significantly affects the total field ($E_{\text{TOTAL}}$). It is noted that $E_1$ and $E_2$ are assumed to have the same phase in the calculation, which is reasonable judging from the simulated field distribution (not shown here for brevity).

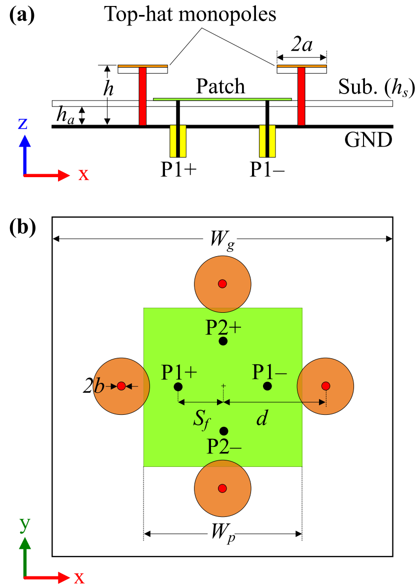


**FIGURE 2.** **Geometry of the proposed antenna: (a) cross-sectional view and (b) top-view. ($W_g$ = 100, $W_p$ = 49.8, $h_a$ = 2.4, $h_s$ = 0.8128, $h$ = 11, $a$ = 6.7, $S_f$ = 18.5, $d$ = 30, $b$ = 1; unit: mm.).**

In the H-plane ($\phi = 90^\circ$), $AF_{\text{monopole}} = 0$, and therefore, the total field of the composite patch-monopole antenna is

$$E_{\text{TOTAL}} = E_{\text{patch}} \tag{5}$$

which indicates that the monopoles theoretically do not affect the H-plane beamwidth of the patch antenna.

One popular concept exploiting the combination of magnetic and electric current sources is magneto-electric (ME) dipoles [23]. These structures are based on Huygen's sources with the target of achieving high-gain unidirectional patterns. Fig. 1 and equations (1)-(4) demonstrate that the concept utilized here is totally different with the aim of broadening the beamwidth. It should be noted that to broaden the beamwidth, an ME dipole needs to be loaded with meta-columns [11] or metallic walls [19], [20] and generally requires more complicated and higher-profile structures.

### B. LOW-PROFILE AND DUAL-POLARIZED DESIGN

The design concept in Fig. 1 has a major drawback of having a high profile due to the monopole length. In order to achieve a low-profile design, we propose the use of top-hat monopoles [24] as shown in Fig. 2(a). Utilizing the structure symmetry, double differential-fed scheme is applied to obtain dual polarization with high isolation (Fig. 2(b)). Roger RO4003 substrate ($\varepsilon_r = 3.38$, tan$\delta = 0.0027$, and $h_s = 0.8128$ mm) is used to print the patch, which is suspended on the GND at an air-gap. For easy realization, the top-hats of monopoles are built on four circular Roger RO4003 pieces with thickness of 0.8128 mm.

Numerical analysis of top-hat monopoles can be found in [25] using the method of moment. The radiation characteristics were shown in [26], which indicates that the radiation

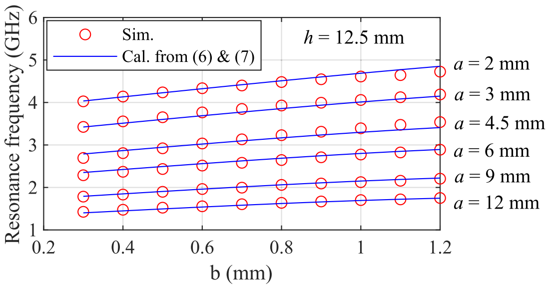


**FIGURE 3.** Simulated and calculated resonance frequency of the top-hat monopole for different values of $a$ and $b$, $h$ is fixed at 12.5 mm.

pattern of a top-hat monopole is equivalent to that of a $\lambda/4$ monopole. Nevertheless, a closed-form formula to estimate the resonance frequency (for initial design parameters) is not available in the literature. To achieve this, we seek an equation for the effective height $h_{\text{eff}}$ of an ideal quarter-wave monopole such that its resonance frequency

$$f_r = \frac{c}{4h_{\text{eff}}} \tag{6}$$

is the same as the resonance frequency of the top-hat monopole characterized by three parameters ($a$, $b$, $h$) (Fig. 2).

Since $h_{\text{eff}}$ can be scaled with ($a$, $b$, $h$), we just need to express $h_{\text{eff}}/h$ as a function of ($a/h$, $b/h$). A wide range of parameters with $a/h \in [0, 1]$ and $b/h \in [0, 0.1]$ is simulated in ANSYS HFSS full-wave simulation. The resonance frequency is defined at which the imaginary part of the input impedance is zero. Applying a simple polynomial curve fitting, an empirical closed-form expression for $h_{\text{eff}}$ is derived as

$$\frac{h_{\text{eff}}}{h} = 1 - 1.9\frac{b}{h} + 3.76\frac{a}{h} - 20.3\frac{ab}{h^2} + 87.1\frac{ab^2}{h^3} \tag{7}$$

It is noted that this equation is chosen such that $h_{\text{eff}} = h$ when $a = b = 0$. Fig. 3 shows the simulated resonance frequency and calculated ones using (6) and (7). The results demonstrate that the proposed empirical equations are reasonably accurate for the range $a/h \in [0, 1]$ and $b/h \in [0, 0.1]$. Using this model, $b = 1$ mm and $h = 11$ mm are first selected, then an initial value for $a$ can be estimated to be about 8 mm to yield a resonance frequency at about 2.5 GHz. Since in the realization, the top-hat monopoles are built on Roger RO4003 pieces, $a$ should be chosen slightly smaller. The final parameter-tuning gives $a = 6.7$ mm. A lower value of $h$ would result in a larger $a$ and slightly degrade the beamwidth. All other optimized parameters are given in the caption of Fig. 2.

### C. BANDWIDTH AND BEAMWIDTH ENHANCEMENTS

Fig. 4 shows 3 design configurations: Ant. 1 is a square patch only; Ant. 2 is the patch loaded with four conventional monopoles; Ant. 3 is the proposed design. For a fair comparison, all designs are optimized with the same GND size, substrate size and center frequency. For impedance matching, the feeding points and the patch size of Ant. 1 are slightly modified as compared to the proposed antenna, i.e., $S_f = 7.5$ mm and $W_p = 47.8$ mm. Referring to Fig. 2, the design parameters of Ant. 2 are as follows: $W_p = 46.4$, $h = 24.6$, $S_f = 15$, $d = 24.5$, $a = 1$, $b = 1$; (unit: mm). Their differential S-parameters are calculated as in [27]. It is noted that due to the perfect symmetry, the antennas yield a theoretically infinite isolation ($S_{dd21} = 0$). As shown in Fig. 4(b), the conventional patch yields a single resonance at 2.5 GHz, whereas Ant. 2 and Ant. 3 show broadband characteristics with two resonances. Fig. 4(c) shows the significant improvement in the beamwidth of Ant. 2 and 3 compared to Ant. 1. For the reflection coefficients of Ant. 2 and 3, the upper resonance is due to the patch and the lower resonance is due to the monopole. This is confirmed by the parametric study shown in Fig. 5.

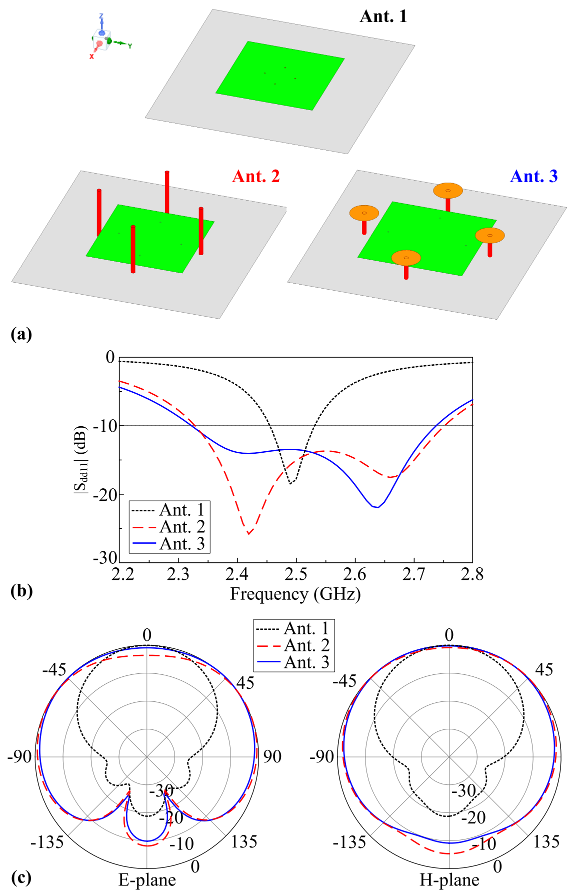


**FIGURE 4.** (a) Steps of design evolution and their simulated (b) $|S_{dd11}|$ and (c) 2.5-GHz normalized radiation patterns.

For the H-plane, the analysis in Section II-A shows that the monopoles do not affect this beamwidth with an infinite GND. To investigate further, the simulated E- and H-plane HPBWs versus the GND size are shown in Fig. 6. It is observed that for $W_g$ at $0.5\lambda_c - 1.5\lambda_c$ ($\lambda_c$ is the free space wavelength referring to the center frequency), the GND size is impactful on improving the HPBW. The $W_g$ of $\sim 0.8\lambda_c$ offers the widest HPBW in both E- and H-planes. As $W_g$ increases

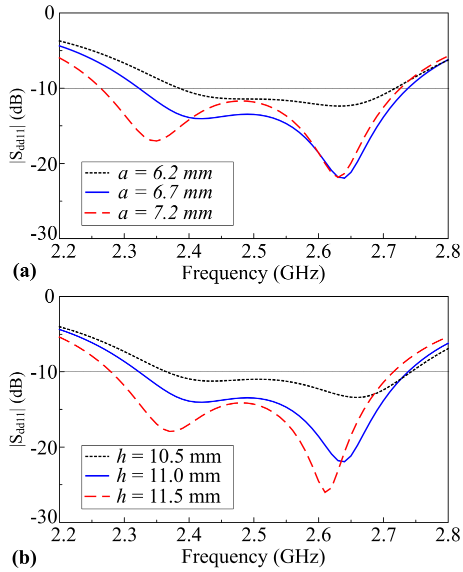


**FIGURE 5.** $|S_{dd11}|$ **of the composite patch-monopole antenna for different values of** ***a*** **and** ***h*****.**

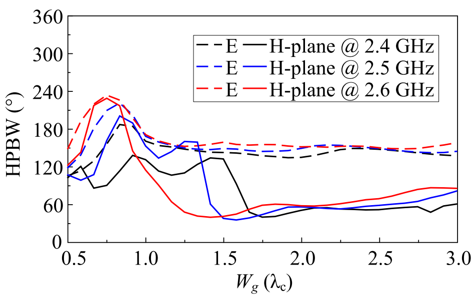


**FIGURE 6.** **HPBWs of the proposed antenna versus the GND size (**$W_g$**).**

beyond 1.5$\lambda_c$, the beamwidths approach the theoretical values with the assumption of infinite GND, i.e., 150° and 70° in the E- and H-planes, respectively.

Although the H-plane beamwidth approaches 70° when the ground size goes to $\infty$, the proposed structure still has a positive impact on enlarging the H-plane beamwidth. This is due to the presence of top-hat monopoles which change the GND structure. From Fig. 6, it provides a wide range values of ground plane size, i.e., $0.5\lambda_c - 1.5\lambda_c$, such that a wide beam (HPBW of about 120°) is achieved. It is noted that a patch alone (without monopoles) can only achieve up to about 85° HPBW in H-plane with a finite ground plane [28].

## III. FABRICATION AND MEASUREMENT

For measurement, the double differential feed is implemented using two out-of-phase power dividers [29]. Roger RO4003 substrate ($\varepsilon_r = 3.38$, $\tan\delta = 0.0027$, and thickness of 0.508 mm) is used to realize the feeding network. Fig. 7 shows a prototype with overall size of 100 mm × 100 mm × 11.5 mm. Its S-parameters are illustrated in Fig. 8(a). The measurements yield a 10-dB return loss bandwidth of 13.8% (2.36 - 2.71 GHz) and an isolation of ≥ 43 dB. Across the

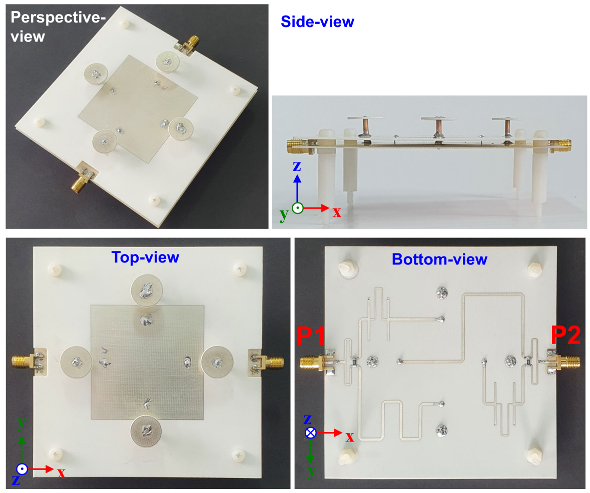


**FIGURE 7.** **Fabricated prototype of the proposed antenna.**

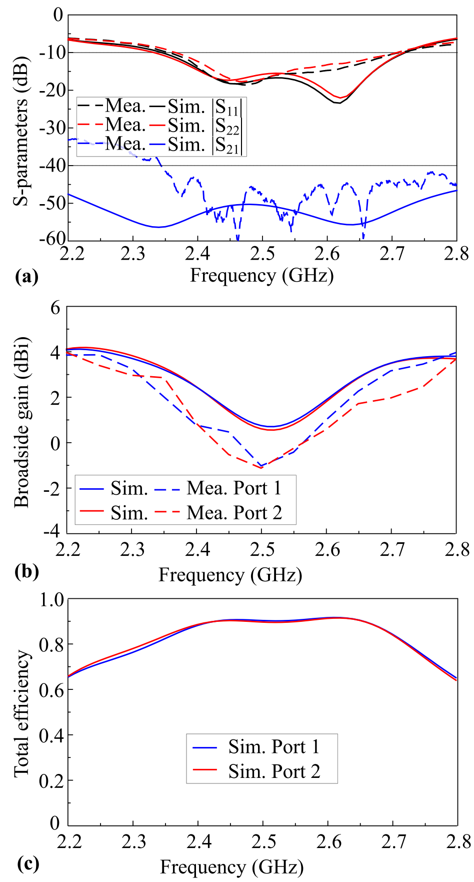


**FIGURE 8.** **(a) S-parameters, (b) realized broadside gains, and (c) total efficiencies of the prototype.**

impedance bandwidth, the measured broadside gains range from −1.1 dBi to 3.2 dBi, which are close to the simulated values of 0.6 - 3.7 dBi (Fig. 8(b)). There is a drop in the broadside gain at the center frequency becuase of the antenna yields the widest beamwidth in both E- and H-planes. A slight discrepancy between the measured and simulated results is attributed to the fabrication tolerances and the imperfect

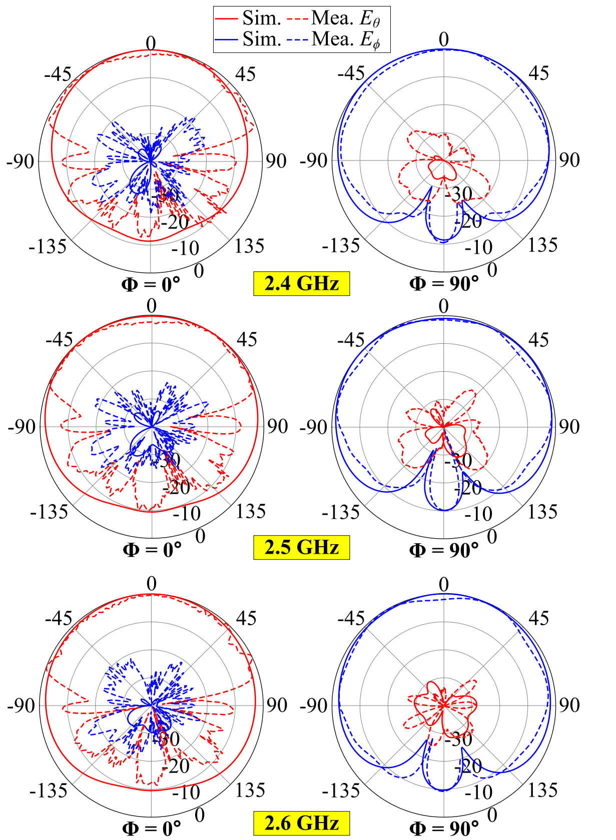


**FIGURE 9.** Normalized radiation pattern of the antenna when P1 is excited.

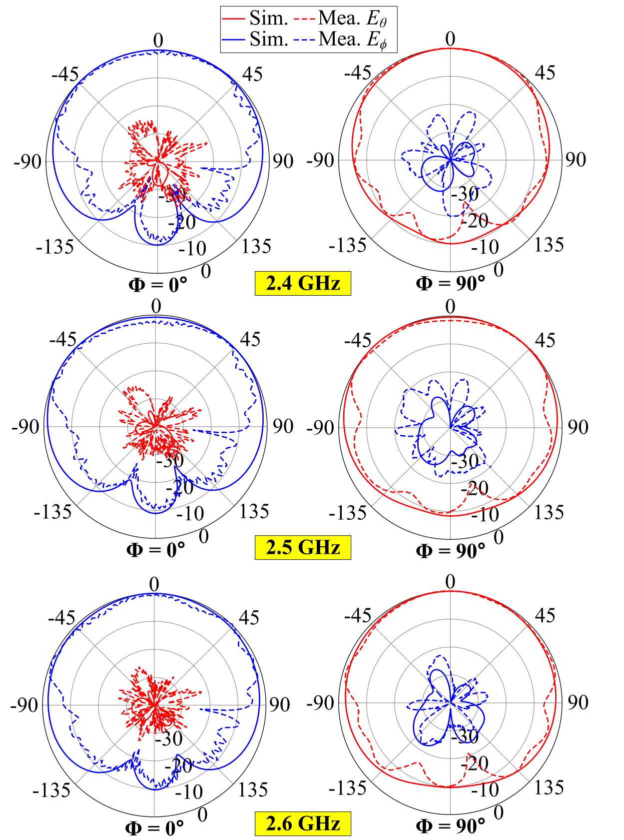


**FIGURE 10.** Normalized radiation pattern of the antenna when P2 is excited.

**TABLE 1.** Comparison of the proposed antenna and the related works.

| Ant. | Overall size ($\lambda_c$) | BW (%) | Pol. | X-Pol. (dB) | Max. HPBW E-plane | Max. HPBW H-plane |
|---|---|---|---|---|---|---|
| [2] | 1.2×1.2×0.22 | 5.0 | LP | -20 | 150° | NA |
| [3] | 0.7×0.7×0.185 | 3.3 | CP | - | 156° | 137° |
| [4] | 2.4×2.4×0.365 | 7.0 | LP | -25 | 90° | 90° |
| [5] | 0.88×0.88×0.20 | 4.3 | LP | -20 | 240° | 110° |
| [8] | 2.85×2.85×0.684 | 10.5 | Dual | -40 | 100° | 100° |
| [10] | 0.6×0.6×0.154 | 25.0 | Dual | -22 | 92° | 110° |
| [12] | 0.58×0.58×0.26 | 28.6 | Dual | -30 | 150° | 168° |
| [17] | 0.94×0.94×0.11 | 12.8 | Dual | - | 102° | 102° |
| [19] | 0.78×0.78×0.2 | 13.3 | Dual | -15 | 90° | 85° |
| Prop. | 0.83×0.83×0.096 | 13.8 | Dual | -30 | 186° | 164° |

BW: operational bandwidth; LP: linear polarization; CP: circular polarization; $\lambda_c$ is the free space wavelength referring to the center frequency.

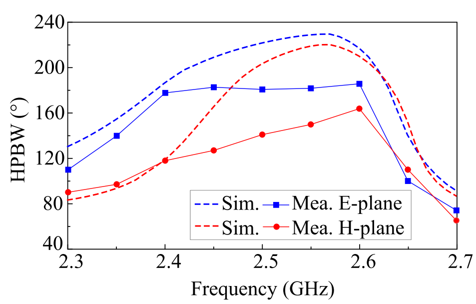


**FIGURE 11.** E- and H-plane HPBWs of the antenna when Port 1 is excited.

chamber. Due to function limitation of the anechoic chamber, the efficiencies of the antenna have not been measured. As shown in 8(c), the simulations result in a total efficiency of greater than 80% and a peak value of 92% for both P1 and P2 excitation.

The normalized patterns in Figs. 9 and 10 demonstrate an excellent widebeam dual-polarized radiation; i.e., with symmetric pattern and cross-polarization level of $\leq -30$ dB at broadside. Fig. 11 shows the HPBWs versus frequency. At 2.4 - 2.6 GHz, the measured HPBWs are in the range of 178° − 186° and 118° − 164° in the E- and H-planes, respectively, whereas the simulated corresponding values are 186° − 230° and 118° − 220°. The measured HPBWs are less than the simulated values which are attributed to the imperfection of the measurement setup, especially toward the back of the antenna.

As compared to other composite patch-monopole antennas [2], [3], [4], [5] (Table 1), the proposed design shows distinct advantages in terms of bandwidth, cross-pol and most importantly, antenna profile (which is the main contribution of this paper). For the beamwidth, compared to [5], the max HPBW in E-plane is smaller, but this is mainly due to our measurement limitation in the $\theta > 90°$-range (the simulated value is 230°). Relative to the widebeam dual-polarized antennas with asymmetric feeding structures [10], [17], [19], the proposed antenna with structural symmetry and differential feed achieves a lower cross-polarization, and consequently a higher port-to-port isolation. It is noted that our preliminary design in [12] is a composite dipole-monopole antenna, where the broadbeam is achieved from the radiation of an equivalent loop electric current. In terms of structure, the antenna in [12] is extremely complicated with many components, multi-layered substrates, and especially suffers from a high profile. The E-plane HPBW in [12] is also smaller than what is presented here.

## IV. CONCLUSION

A dual-polarized patch antenna with broadband and wide-beam characteristics has been presented. The effect of the loading monopoles is investigated thoroughly. Empirical equation for the resonance frequency of a top-hat monopole is proposed for a quick estimation of the initial design parameters. Structure symmetry is utilized to achieve very high-isolation dual-polarization radiation. Many advantages, including low-profile, simple configuration, broadband, dual-polarization, high isolation and widebeam, make the proposed antenna a good candidate for wireless local area network, 5G in-door access-points, as well as other modern wireless communication systems.

## REFERENCES


[1] Y. Li, S. Xiao, and J. Guo, "A review of wideband wide-angle scanning 2-D phased array and its applications in satellite communication," *J. Commun. Inf. Netw.*, vol. 3, no. 1, pp. 21–30, Mar. 2018, doi: 10.1007/s41650-018-0001-x.

[2] N. Kuga and H. Arai, "Feeding condition of patch-monopole composite antenna with horizontal broad beam," in *Proc. Asia–Pacific Microw. Conf. (APMC)*, vol. 3, 2001, pp. 1358–1361.

[3] C. Wu, L. Han, F. Yang, L. Wang, and P. Yang, "Broad beamwidth circular polarisation antenna: Microstrip-monopole antenna," *Electron. Lett.*, vol. 48, no. 19, pp. 1176–1178, Sep. 2012.

[4] U. A. Pawar, S. Chakraborty, T. Sarkar, A. Ghosh, L. L. K. Singh, and S. Chattopadhyay, "Quasi-planar composite microstrip antenna: Symmetrical flat-top radiation with high gain and low cross polarization," *IEEE Access*, vol. 7, pp. 68917–68929, 2019.

[5] K. Sun, S. Liu, Y. Chen, Y. Zhao, and D. Yang, "Design of composite microstrip-monopole antenna with 180° 1 db beamwidth based on complementary sources concept," *IEEE Antennas Wireless Propag. Lett.*, vol. 20, no. 8, pp. 1577–1581, Aug. 2021.

[6] R. A. Alhalabi and G. M. Rebeiz, "High-efficiency angled-dipole antennas for millimeter-wave phased array applications," *IEEE Trans. Antennas Propag.*, vol. 56, no. 10, pp. 3136–3142, Oct. 2008.

[7] S. X. Ta, H. Choo, and I. Park, "Broadband printed-dipole antenna and its arrays for 5G applications," *IEEE Antennas Wireless Propag. Lett.*, vol. 16, pp. 2183–2186, 2017.

[8] M. Mirmozafari, G. Zhang, S. Saeedi, and R. J. Doviak, "A dual linear polarization highly isolated crossed dipole antenna for MPAR application," *IEEE Antennas Wireless Propag. Lett.*, vol. 16, pp. 1879–1882, 2017.

[9] M. Mirmozafari, S. Saeedi, G. Zhang, and Y. Rahmat-Samii, "A crossed dipole phased array antenna architecture with enhanced polarization and isolation characteristics," *IEEE Trans. Antennas Propag.*, vol. 68, no. 6, pp. 4469–4478, Jun. 2020.

[10] Z. Zhang, Y. Zhao, D. Wu, S. Zuo, L. Ji, X. Yang, and G. Fu, "Dual-polarised crossed-dipole antenna with improved beamwidth," *IET Microw., Antennas Propag.*, vol. 12, no. 6, pp. 890–894, May 2018.

[11] B. Feng, L. Li, K. L. Chung, and Y. Li, "Wideband widebeam dual circularly polarized magnetoelectric dipole antenna/array with meta-columns loading for 5G and beyond," *IEEE Trans. Antennas Propag.*, vol. 69, no. 1, pp. 219–228, Jan. 2021.

[12] L. Thi Cam Ha, S. X. Ta, N. X. Quyen, N. K. Kiem, and D.-N. Chien, "High-isolation wide-beam dual-polarized antenna utilizing symmetrical feeding," *Prog. Electromagn. Res. M*, vol. 111, pp. 53–63, 2022.

[13] C.-M. Liu, S.-Q. Xiao, H.-L. Tu, and Z. Ding, "Wide-angle scanning low profile phased array antenna based on a novel magnetic dipole," *IEEE Trans. Antennas Propag.*, vol. 65, no. 3, pp. 1151–1162, Mar. 2017.

[14] Y. He and Y. Li, "Dual-polarized microstrip antennas with capacitive via fence for wide beamwidth and high isolation," *IEEE Trans. Antennas Propag.*, vol. 68, no. 7, pp. 5095–5103, Jul. 2020.

[15] M. Boyuan, J. Pan, S. Huang, D. Yang, and Y. Guo, "Wide-beam dielectric resonator antennas based on the fusion of higher-order modes," *IEEE Trans. Antennas Propag.*, vol. 69, no. 12, pp. 8866–8871, Dec. 2021.

[16] S.-J. Sun, Y.-C. Jiao, and Z. Weng, "Wide-beam dielectric resonator antenna with attached higher-permittivity dielectric slabs," *IEEE Antennas Wireless Propag. Lett.*, vol. 19, no. 3, pp. 462–466, Mar. 2020.

[17] G. Yang and S. Zhang, "Dual-polarized wide-angle scanning phased array antenna for 5G communication systems," *IEEE Trans. Antennas Propag.*, vol. 70, no. 9, pp. 7427–7438, Sep. 2022.

[18] G. Yang, J. Li, D. Wei, and R. Xu, "Study on wide-angle scanning linear phased array antenna," *IEEE Trans. Antennas Propag.*, vol. 66, no. 1, pp. 450–455, Jan. 2018.

[19] J. Y. Yin and L. Zhang, "Design of a dual-polarized magnetoelectric dipole antenna with gain improvement at low elevation angle for a base station," *IEEE Antennas Wireless Propag. Lett.*, vol. 19, no. 5, pp. 756–760, May 2020.

[20] B. Feng, J. Lai, and C.-Y.-D. Sim, "A building block assembly dualband dual-polarized antenna with dual wide beamwidths for 5G microcell applications," *IEEE Access*, vol. 8, pp. 123359–123368, 2020.

[21] R.-Y. Li, Y.-C. Jiao, Y.-X. Zhang, L. Zhang, and H.-Y. Wang, "A DRA with engraved groove and comb-like metal wall for beamwidth enhancement in both E- and H-planes," *IEEE Antennas Wireless Propag. Lett.*, vol. 20, no. 4, pp. 543–547, Apr. 2021.

[22] C. Balanis, *Antenna Theory: Analysis and Design*. Hoboken, NJ, USA: Wiley, 2015. [Online]. Available: https://books.google.com.vn/books?id=PTFcCwAAQBAJ

[23] M. Li and K.-M. Luk, *Wideband Magneto-Electric Dipole Antennas*. Singapore: Springer, 2014, pp. 1–43.

[24] V. Trainotti and L. A. Dorado, "Short low- and medium-frequency antenna performance," *IEEE Antennas Propag. Mag.*, vol. 47, no. 5, pp. 66–90, Oct. 2005.

[25] T. L. Simpson, "The disk loaded monopole antenna," *IEEE Trans. Antennas Propag.*, vol. 52, no. 2, pp. 542–550, Feb. 2004.

[26] Z. Shen and J. Wang, "Top-hat monopole antenna for conical-beam radiation," *IEEE Antennas Wireless Propag. Lett.*, vol. 10, pp. 396–398, 2011.

[27] B. R. Eisenstadt, B. Stengel, and B. M. Thompson, *Microwave Differential Circuit Design Using Mixed-Mode S-Parameters*. Norwood, MA, USA: Artech House, 2006.

[28] M. Tuan Nguyen, B. Kim, H. Choo, and I. Park, "Effects of ground plane size on a square microstrip patch antenna designed on a low-permittivity substrate with an air gap," in *Proc. Int. Workshop Antenna Technol. (iWAT)*, Mar. 2010, pp. 1–4.

[29] Z.-Y. Zhang, Y.-X. Guo, L. C. Ong, and M. Y. W. Chia, "A new wide-band planar balun on a single-layer PCB," *IEEE Microw. Wireless Compon. Lett.*, vol. 15, no. 6, pp. 416–418, Jun. 2005.


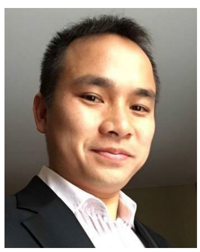

**SON XUAT TA** (Member, IEEE) received the B.Sc. (Eng.) degree in electronics and telecommunications from the Hanoi University of Science and Technology, Vietnam, in August 2008, and the Ph.D. degree in electrical engineering from Ajou University, South Korea, in February 2016. From March 2016 to February 2017, he was a Postdoctoral Research Fellow with the Department of Electrical and Computer Engineering, Ajou University. From March 2017 to August 2017, he was with the Division of Computational Physics, Institute for Computational Science, and the Faculty of Electrical and Electronics Engineering, Ton Duc Thang University, Ho Chi Minh City, Vietnam. Since September 2017, he has been a Lecturer with the School of Electronics and Telecommunication (now renamed as the School of Electrical and Electronic Engineering), Hanoi University of Science and Technology. He has authored and coauthored more than 100 technical journal and conference papers. His research interests include antennas, metamaterials, metasurfaces, metamaterial-based antennas, metasurface-inspired antennas, circularly polarized antennas, and millimeter-wave antennas. He served as a reviewer for more than 15 scientific journals. He has been selected as a Top Reviewer of IEEE TRANSACTIONS ON ANTENNAS AND PROPAGATION, in 2020, 2021, and 2022.

**THANH TUNG PHUNG** is currently pursuing the B.Sc. (Eng.) degree in electronic and telecommunication engineering from the Hanoi University of Science and Technology (HUST), Vietnam. Since 2021, he has been a Internship Researcher with the Communication Research and Development Laboratory (CRD-Lab), HUST. His research interests include microstrip patch antennas, dual-polarized antennas, multiband antennas, and reconfigurable antennas.

**KHAC KIEM NGUYEN** (Member, IEEE) was born in Hanoi, Vietnam, in 1978. He received the B.Eng., M.Sc., and Ph.D. degrees from the School of Electronics and Telecommunication (SET) [now renamed as the School of Electrical and Electronic Engineering (SEEE)], Hanoi University of Science and Technology (HUST), Vietnam, in 2001, 2003, and 2017, respectively. Since 2001, he has been a Lecturer with SEEE, and a Researcher with CRD LAB, HUST. His research interests include design microstrip antenna for next generation mobile communication systems and passive RF components.

**CHIEN DAO-NGOC** (Senior Member, IEEE) received the Dipl. Eng. degree from the School of Electronics and Telecommunication (SET), Hanoi University of Science and Technology, Vietnam (HUST), in 1997, and the M.Sc. and Ph.D. degrees from the Department of Electronics and Computer Engineering, Gifu University, Japan, in 2002 and 2005, respectively.

From April 2005 to October 2011, he was a Senior Lecturer with SET, HUST, and appointed as the Director of the Centre for Research and Development on Satellite Navigation Technology, South East Asia, in 2009. He has been an Associate Professor, since November 2010. Since November 2011, he has been with the Department of High Tech., Ministry of Science and Tech., Vietnam, and appointed as an Adjunct Professor with SET, HUST. His research interests include computational electromagnetics based on MoM and FDTD method and analysis and design of modern antenna and of nanometric integrated optical circuits based on surface plasmon polaritons. He has been a reviewer of several journals/transactions of *Journal of the Optical Society of America A* (OSA), IEEE, Elsevier, and American Geophysical Union (AGU) and numerous of technical and science conferences.

**NGHIA NGUYEN-TRONG** (Senior Member, IEEE) received the Ph.D. degree (Hons.) in electrical engineering from The University of Adelaide, Adelaide, SA, Australia, in 2017.

He is currently a Lecturer with The University of Adelaide. His research interests include microwave circuits, advanced materials, absorbers, and various types of antennas.

Dr. Nguyen-Trong was one of a recipients of the Best Student Paper Award from the 2014 IWAT, the 2015 IEEE MTT-S NEMO, the 2017 ASA Conferences, and the Best Paper Award from AMS Conference, in 2018 and 2020. He has been continuously selected as a Top Reviewer of IEEE Transactions on Antennas and Propagation, in 2018, 2019, 2020, and 2021; and IEEE Antennas and Wireless Propagation Letters, in 2018 and 2021. He serves as the Technical Co-Chair for the 2020 Australian Microwave Symposium (AMS) and the 2022 IEEE International Symposium on Antennas and Propagation. He is listed among Australia's Top 40 Early Career Researchers by The Australian, in November 2021.